C. R. Mecanique 340 (2012) 230–246

Contents lists available at SciVerse ScienceDirect

Comptes Rendus Mecanique

www.sciencedirect.com

Recent Advances in Micromechanics of Materials

Various estimates of Representative Volume Element sizes based on a statistical analysis of the apparent behavior of random linear composites

Moncef Salmi [a], François Auslender [a], Michel Bornert [b,*], Michel Fogli [a]

[a] Mechanical Engineering Research Group, Blaise Pascal University/IFMA, BP 265, 63175 Aubière, France
[b] Laboratoire Navier, Université Paris-Est, École des Ponts ParisTech, Champs-sur-Marne, 77455 Marne-la-Vallée cedex, France

ARTICLE INFO

Article history:
Available online 29 March 2012

This thematic issue of the *Comptes Rendus Mécanique*, devoted to *Heterogeneous Materials and Composites*, is dedicated to A. Zaoui

Keywords:
RVE size
Apparent behavior
Fluctuations
Random linear composites

ABSTRACT

This article aims at proposing various estimates of the size of the Representative Volume Element (RVE) of random linear elastic matrix–inclusion composites. These estimates are derived from the computation of the apparent behavior of finite size volume elements (VE) by a new procedure presented in [18] by Salmi et al. (2012) and briefly recalled. Two different points of view to define an RVE are considered: the RVE is defined as being the smallest VE required either to evaluate numerically the considered effective property of the composite by appropriate statistical averaging of apparent ones, or to be allowed to replace any instance of the heterogeneous material by a unique homogeneous equivalent one in structural mechanics problems. In order to introduce the fluctuations of the apparent properties within such definitions of the RVE size, we first study the statistics of the apparent properties. Then, relying on the results of this statistical study, several proposals of RVE criteria are presented and applied to random linear elastic fiber–matrix composites for several contrasts and inclusion (or pore) volume fractions.

1. Introduction

For structural calculations where CPU time and memory are issues of concern, it is appealing to describe the behavior of the volume elements (VEs) of a composite material as being homogeneous with constant overall properties. To this end, the concept of representative volume element (RVE) is of paramount importance, especially when numerical simulations are used to determine the expected effective properties. Many definitions of an RVE are available in the literature. Hill [1], in his pioneering work on the effective elastic properties of reinforced composites, defined the RVE as "a sample that (a) is structurally entirely typical of the whole mixture on average, and (b) contains a sufficiently large number of inclusions for the apparent overall moduli to be effectively independent of surface values of traction and displacement, as long as these values are macroscopically uniform". Such a definition combines two major ideas behind the concept of RVE: the statistical representativity of the microstructure and the independence of its apparent behavior with respect to details of the boundary conditions (BC) applied to it, as long as their averages are uniform at some larger scale. This last concept of so-called "macrohomogeneous" loading conditions is associated with a decomposition of the variations of the mechanical loading conditions on two clearly separated length scales. Such a principle of separation of length scales has later been announced again by Hashin [2] for whom "the RVE should be large enough to contain sufficient information about the microstructure in order to be representative, however it should be much smaller than the macroscopic body". Hill's definition supplements this principle by a pronouncement on the independence of the apparent behavior with respect to BC, defining this way a unique

* Corresponding author.
E-mail addresses: moncef.salmi@ifma.fr (M. Salmi), francois.auslender@univ-bpclermont.fr (F. Auslender), michel.bornert@enpc.fr (M. Bornert), michel.fogli@univ-bpclermont.fr (M. Fogli).

1631-0721/$ – see front matter
doi:10.1016/j.crme.2012.02.007

effective behavior. These definitions are in essence only qualitative and no practical procedure to determine their extension is proposed. An important character is however that they consider only a single realization of the heterogeneous composite and conditions that allow to replace it by an equivalent effective homogeneous medium. The conditions for the existence of such an effective behavior have later been investigated from a theoretical point of view by several authors. As pointed out by Ostoja-Starzewski [3] "the RVE is clearly defined in two situations only": (i) unit cell in a periodic microstructure [4], (ii) a volume containing a very large (mathematically infinite) set of micro-scale element (e.g. grains), possessing statistically homogeneous and ergodic properties [5,6]. The present article will be focused on the second situation.

Instead of considering only one instance of the heterogeneous material, one may alternatively consider a composite as a statistical process and focus attention on effective properties that link ensemble averages of mechanical fields, without paying attention to fluctuations of individual apparent properties. This second perspective is taken by Drugan and Willis [7] who define the RVE as "the smallest material volume element of the composite for which the usual spatially constant overall modulus macroscopic representation is a sufficiently accurate model to represent mean constitutive response". Their definition of the RVE opens a way to evaluate analytically its size [7–9]. Indeed, they establish a nonlocal constitutive equation relating the ensemble average of the stress and strain for random linear composites and produce quantitative estimates of the minimum RVE size by comparing the magnitude of the nonlocal to local terms in the constitutive equation when the ensemble average strain loading is spatially varying.

A third, more practical, point of view for the definition of the RVE and more precisely its size, is linked with the determination of the effective properties of a heterogeneous material by the combination of unit cell-type calculations and Monte Carlo simulations of their microgeometries (e.g. [10–16]). The question is to evaluate the minimal size of a computational volume element (VE) such that the average of its apparent behavior evaluated for a sufficiently large number of realizations of its microgeometry converges to the wanted effective behavior. As a typical instance of this type of approaches, Kanit et al. in [13] made use of the notion of integral range and confidence interval to derive a closed-form relation between the relative error associated with the wanted effective property and both the size of the VE and the number of realizations. This relation allows one to predict the number of virtual samples of a given size necessary to reach a given level of accuracy and conversely to predict the relative accuracy for a given number of realizations. Applying their procedure to linear random two-phase composites, Kanit et al. clearly showed that the size of the RVE, defined this way, not only depends on the microgeometry (i.e. its morphology and volume fractions) of the composite, but also on the investigated physical property, the contrast between the constitutive phases, and above all, a given accuracy in the prediction of the effective property.

The above-mentioned definitions and analyses — as well as other definitions reviewed in Gitman et al. [17] — lead to various RVE sizes, even for a same given material property, accuracy and similar morphology. For instance, for linear elastic random disk–matrix reinforced composites, Ostoja-Starzewski [11] found large RVE sizes, 10 to 50 times a single inclusion, with a relative error of 5% at a contrast between the phases moduli ranging from 10^2 to 10^4 for a reinforcement volume fraction of 20%. At the opposite end of the range of proposed RVE sizes, Drugan and Willis [7] derived for the same type of composite — however reinforced by spherical inclusions — and for the same accuracy an RVE size approximatively equal to only two reinforcement diameters for any contrast and for all reinforcement volume fractions up to 40%. The quantitative differences in the results obtained from the above-mentioned analysis is the result of the existence of various points of view and definitions of the concept of RVE, which is still an issue of concern and requires more investigations.

The present article aims at applying some of the above described concepts of RVE and at proposing extensions of previously proposed RVE criteria for a particular class of matrix–inclusion random composites for which a new procedure to compute sharp upper and lower bounds for the effective linear elastic properties has recently been proposed by Salmi et al. [18]. The new bounds rely on a strategy which is inspired both by the work of Huet [19] — the bounds are obtained by performing ensemble averages of their apparent elastic moduli computed with either affine displacement boundary conditions (ADBC) or uniform traction boundary conditions (UTBC) — and by the one of Danielson et al. [20] — the apparent elastic moduli are now defined on non-square instead of square VEs made of an assemblage of Voronoï cells, each cell being composed of a single inclusion surrounded by matrix (see Fig. 1). It is shown in [18] that these new bounds converge quickly with the VE size, even for infinite contrasts unlike the classical ones derived by Huet [19,11] for square VEs. The presented work aims at defining new RVE criteria relying on the new scheme developed in [18]. For that, two different points of view to define an RVE will be considered. The first one aims to determine the minimum VE size required to evaluate the effective properties of a heterogeneous material. The RVE criteria provided in [19,11,3,7,10,13,17] are instances of such computational RVEs. The second viewpoint considers that the RVE size is reached when one is allowed to replace a heterogeneous material by an equivalent one in structural mechanics problems. This type of RVE criteria requires that the separation of scale principle must be fulfilled. Hill [1] and Hashin [2] RVE definitions illustrate this second viewpoint. Both these viewpoints define an RVE by means of qualitative arguments only. To go further, we need to introduce quantitative considerations. For that, it is often useful to know, at least partially, the statistics of the apparent properties in order to quantify not only their mean values but also their scatter. Based on these considerations, a statistical study of the apparent properties computed by means of the new approach developed in Salmi et al. [18] is performed. Relying on the trends derived from this study, some proposals to define RVE sizes are then presented.

The structure of this article is as follows. In Section 2, the procedure elaborated in [18] to derive new bounds for the effective behavior of random linear elastic matrix–inclusion composites from weighted ensemble averages of the apparent properties computed on non-square VEs is briefly recalled. Section 3 is dedicated to the study of the statistics of these apparent behaviors computed on non-square Voronoï-type VEs subjected to either ADBC or UTBC. This statistical study is

carried out for two-phase composites composed of a matrix and aligned identical cylindrical fibers randomly distributed in the transverse plane. From the results of the statistical study, three different RVE criteria are proposed in Section 4. They are applied to the fiber–matrix composite considered in Section 3 for various contrasts and volume fractions. Conclusions are summarized in Section 5.

The tensor notation used herein is a fairly standard one. The orders of the tensors are clear when taken in context. Products containing dots denote summation over repeated Latin indices. Regarding probabilistic aspects, all the random quantities (variables, fields) considered in this work are assumed to be defined on the same probability space $\{\Theta, F, P\}$, where Θ is a sample space, F is a σ-algebra of subsets of Θ and P is a probability on F. For the sake of simplicity, the notation $\xi(\omega)$ will be used to denote both a random variable ξ and its realization for $\omega \in \Theta$. In the same way, $\psi(x, \omega)$ will be used to denote an ω-realization of a random field ψ, its value at position x, as well as the random field itself. Finally, the mathematical expectation and standard deviation of any random variable ξ will be denoted $E(\xi)$ and $\sigma(\xi)$, respectively.

2. New bounds of the effective behavior for matrix–inclusion-type composites

By making use of different arguments, Huet [19] and later Sab [6] independently showed that the arithmetic ensemble average of the apparent stiffness associated with ADBC and the harmonic ensemble average of the apparent stiffness associated with UTBC both applied to square (in 2D) or cubic (in 3D) shaped samples of size L are upper and lower bounds of the effective behavior, respectively. When applied to different types of heterogeneous materials such as matrix–inclusion composites [11,3] or polycrystals [21], it has been numerically checked that these bounds provide good estimates of the effective behavior even for relatively low values of $\delta = L/d$ but only for weak to medium contrast between the constituents of the composite. The micro-scale d refers to the typical size of the constitutive elements of the heterogeneous material (e.g. grain size in a polycrystal, or inclusion or fiber diameter in a composite). For composites with large contrast, e.g. containing rigid particles or pores, simulations performed on planar linear elastic disk–matrix composites [11] have revealed that the discrepancy between the upper and lower bounds of the effective properties remains significant even for large value of δ. This discrepancy is induced by a blow-up of either the upper bound for rigidly reinforced composites or the lower bound for porous materials. This blow-up occurs because the part of the strain energy due to the particles which intersect the edges of the square cell becomes very large when ADBC (resp. UTBC) are directly applied to rigid particles (resp. pores). To avoid such limitations, Salmi et al. [18] considered non-square (or non-cubic) VEs comprised of cells assemblages (e.g. Voronoï cells assemblages), each cell being composed of an inclusion, *strictly located inside the cell*, surrounded by the matrix, thus forbidding any direct application of boundary conditions to particles. By making use of the classical bounding theorems for linear elasticity and appropriate averaging procedures, sharp bounds of the effective behavior are derived from ensemble averages of the apparent behaviors associated with non-square (resp. non-cubic) VEs. As mentioned in the introduction, these new bounds converge quickly with the VE size towards the effective behavior, even for infinite contrasts, thus providing a new numerical approach which might be employed to determine RVE sizes. The principles of this approach are briefly recalled in this section. Since the governing ideas are the same in 2 or 3 dimensions, only 2D situations are considered.

2.1. Non-square VEs

We consider a random microstructure made of K constitutive phases, characterized by a set of K stochastic fields

$$B \in \left\{ \chi^r \in \{0,1\}^{\mathbb{R}^{\mathrm{d}} \times \Theta}, 1 \leqslant r \leqslant K, \sum_{r=1}^{K} \chi^r = 1 \right\}$$

where $\mathrm{d} = 2$ is the space dimension and χ^r the random characteristic functions, being 1 if the position vector x is in phase r, and 0 otherwise. The microstructure B is assumed to be stationary and ergodic. From B, we obtain for each $\omega \in \Theta$ a realization $B(\omega)$ of the composite. In order to design non-square VEs the boundaries of which do not intersect very stiff or very soft phases, the microstructures $B(\omega)$ considered in this article are of the matrix–inclusion type only. Further, it is assumed that no contact occurs between the inclusions which can be of any size and any shape. The new non-square VEs are defined as connex assemblages of elementary cells, each elementary cell being composed of a sole inclusion surrounded by matrix. The cells are not allowed to intersect and their union is supposed to cover the whole microstructure. A possible way to decompose the microstructure into such cells is to associate to any particular inclusion the points in the matrix that are closer to this inclusion than to any other. The boundaries of the cells are then defined as the watershed lines of the distance function to the inclusions [22]. A particular case of practical interest is when the inclusions are disks of the same diameter; the corresponding decomposition coincides then with the classical Voronoï subdivision of the 2D space associated with the disks centers. This situation will be considered in the next section and is illustrated in Fig. 1. Other definitions of cells could however be used.

For such a random microstructure and its decomposition into cells, n non-square VEs of size δ are generated by considering square windows Ω^s_{δ, X_k} of width δ and centered on positions $X^k = (x^k_1, x^k_2)$ $(k = 1, \ldots, n)$, defined by $\Omega^s_{\delta, X_k} = [x_1 - L/2, x_1 + L/2] \times [x_2 - L/2, x_2 + L/2]$, and by extracting, for each window Ω^s_{δ, X_k}, the set of inclusions which have their center of mass inside this window. The non-square domains $\Omega_{\delta, X_k}(\omega)$, of size δ and centered on positions X^k, are

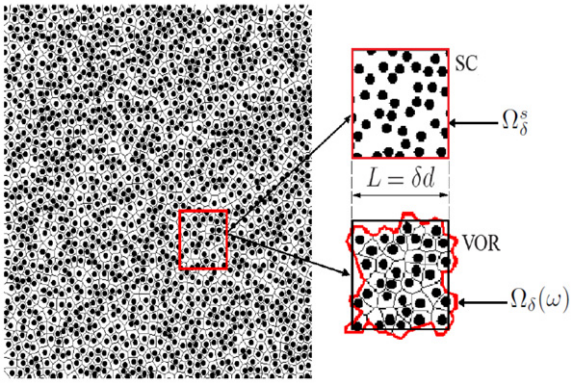

Fig. 1. VEs generation from a large microstructure: square cell (SC) and Voronoï (VOR)-type windows and VEs.

then defined as the unions of the cells associated with these sets of inclusions. See Fig. 1 for a graphical illustration of the construction of the domains Ω^s_{δ,X_k} and $\Omega_{\delta,X_k}(\omega)$. The n VEs, the apparent behaviors of which will be computed to bound the effective properties of the composite, are the restrictions $B_{\delta,X_k}(\omega)$ of a realization of the composite $B(\omega)$ to its corresponding non-square domains $\Omega_{\delta,X_k}(\omega)$. In the following, because of the stationarity of the random set B, the spatial dependence relative to the windows centers X_k will no longer be specified unless required. Note however that in order to avoid any bias in the statistical ensemble averaging of the apparent properties, the centers X_k have to be chosen such that the windows Ω^s_{δ,X_k} (and consequently $\Omega_{\delta,X_k}(\omega)$) do not overlap. They may be placed randomly or on a regular grid.

2.2. Definition of the apparent behavior

In what follows, the outer surface of any domain A and its normal will be denoted by ∂A and $n(x)$, respectively. When the VE $B_\delta(\omega)$ is smaller than the RVE, its apparent behavior depends both on ω and on the prescribed BC on $\partial\Omega_\delta(\omega)$. In linear elasticity, the apparent behaviors of $B_\delta(\omega)$ associated with ADBC — $u(x,\omega) = \bar{\varepsilon}.x, \forall x \in \partial\Omega_\delta(\omega)$ — or with UTBC — $\sigma(x,\omega).n(x) = \bar{\sigma}.n(x), \forall x \in \partial\Omega_\delta(\omega)$ — are, respectively, described by the fourth-order stiffness $C^d_\delta(\omega)$ or compliance $S^t_\delta(\omega)$ tensors. They are defined by

$$\forall \bar{\varepsilon}, \quad V_\delta(\omega)\,\bar{\varepsilon} : C^d_\delta(\omega) : \bar{\varepsilon} = \inf_{u \in K_\delta(\bar{\varepsilon},\omega)} \int_{\Omega_\delta(\omega)} \varepsilon\big(u(x)\big) : C(x,\omega) : \varepsilon\big(u(x)\big)\,\mathrm{d}x$$
$$\text{with } K_\delta(\bar{\varepsilon},\omega) = \big\{u(x)/u(x) = \bar{\varepsilon}.x\ \forall x \in \partial\Omega_\delta(\omega)\big\} \tag{1}$$
$$\forall \bar{\sigma}, \quad V_\delta(\omega)\bar{\sigma} : S^t_\delta(\omega) : \bar{\sigma} = \inf_{\sigma \in S_\delta(\bar{\sigma},\omega)} \int_{\Omega_\delta(\omega)} \sigma(x) : S(x,\omega) : \sigma(x)\,\mathrm{d}x$$
$$\text{with } S_\delta(\bar{\sigma},\omega) = \big\{\sigma(x)/\operatorname{div}\big(\sigma(x)\big) = 0\ \forall x \in \Omega_\delta(\omega); \sigma(x).n(x,\omega) = \bar{\sigma}.n(x,\omega)\ \forall x \in \partial\Omega_\delta(\omega)\big\} \tag{2}$$

In Eqs. (1) and (2) as well as hereafter, the superscripts d and t refer to ADBC and UTBC, respectively. The random variable $V_\delta(\omega)$ denotes the volume of the domain $\Omega_\delta(\omega)$. The tensors $C(x,\omega)$ and $S(x,\omega)$ are the local stiffness and compliance associated with an ω-realization of the composite. In the sequel, they are assumed to be defined by

$$C(x,\omega) = \sum_{r=1}^{K} C^r \chi^r(x,\omega), \qquad S(x,\omega) = \sum_{r=1}^{K} S^r \chi^r(x,\omega) \tag{3}$$

where C^r (resp. S^r) is the non-random stiffness (resp. compliance) tensor of phase r.

For ergodic and stationary materials, Papanicolaou [5] and later Sab [6] have shown that

$$\lim_{\delta\to\infty} C^d_\delta(\omega) = \lim_{\delta\to\infty} S^t_\delta(\omega) = C^{eff} = \big(S^{eff}\big)^{-1} \tag{4}$$

thus defining the effective behavior C^{eff} which does not depend on either the BC or the realization ω. In practice, Eq. (4) is satisfied, at a specified accuracy, for δ greater than a critical size δ_c which, according to the viewpoint adopted by Hill [1], may be interpreted as one possible definition of the RVE size, as discussed in Section 4.

2.3. Order relations for the apparent tensor moduli

Relying on the non-regular VEs defined in Section 2.1 and considering stationary and ergodic matrix–inclusion composites, Salmi et al. [18] recently derived new bounds of the effective behavior stemming from weighted ensemble average of the apparent properties. The obtained bounds — referred to as the VOR bounds in the sequel — are defined by

$$C_\delta^{VOR+} = E\left(\frac{V_\delta}{E(V_\delta)} C_\delta^d\right), \qquad C_\delta^{VOR-} = E\left(\frac{V_\delta}{E(V_\delta)} S_\delta^t\right)^{-1} \tag{5}$$

and satisfy the following order relations:

$$\forall \delta \in \mathbb{R}^+, \quad C_{\delta'}^{VOR-} \leqslant C_\delta^{VOR-} \leqslant \left(S^{eff}\right)^{-1} = C^{eff} \leqslant C_\delta^{VOR+} \leqslant C_{\delta'}^{VOR+} \quad \text{for } \delta' = \delta/2 \tag{6}$$

In Eq. (6) and in what follows, the inequality $A \leqslant B$ between two fourth-order tensors A and B should be understood in the sense of quadratic form, i.e. $t : A : t \leqslant t : B : t$ for any second-order tensor t. The proof of Eq. (6) is given in [18]. Briefly, Salmi et al. derive relation (6) by making use of the classical energy bounding theorems and appropriate averaging procedures. Stationarity and ergodicity of the microstructure are required in the proof. A key point is to notice that the volume $V_\delta(\omega)$ of the non-square VE $B_\delta(\omega)$ is a random variable unlike in Huet's approach [19] based on square VEs where $V_\delta^s = |\Omega_\delta^s| = (\delta d)^2$ is a constant. When applying Eqs. (5) and (6) to such square VEs, the bounds and order relations derived by Huet [19] and later by Sab [6] are recovered straightforwardly.

As shown in Eq. (5), the VOR bounds are defined as weighted ensemble averages of the apparent properties. In what follows, for ease of notation the weight $\frac{V_\delta}{E(V_\delta)}$ associated with each ω-realization of the apparent properties will be omitted in the expectation unless required, i.e. $E(\frac{V_\delta}{E(V_\delta)} C_\delta^d) \equiv E(C_\delta^d)$. The same weights are used later on for the computation of standard deviations and probability density functions relative to VOR-type quantities.

Salmi et al. have shown in [18] that the VOR bounds converge quickly towards the effective behavior and improve on the classical Huet's bounds for all contrasts and particle volume fractions. Therefore, they can be used to evaluate RVE sizes. In contrast to other numerical studies of RVE sizes [13] which are based on *estimates* of effective properties, the present work relies on *exact and efficient bounds*. The efficiency of the bounds is mainly due to the fact that the matrix–inclusion nature of the microstructure is well taken into account. In essence, the proposed approach is an adaptation of the Morphologically Representative Pattern-based approach [23] which leads to efficient bounds for similar matrix–inclusion microstructures which strongly improve on more general ones [24].

More generally, the entire statistics of the apparent behaviors $C_\delta^d(\omega)$ and $S_\delta^t(\omega)$ defined on non-square Voronoï-type VEs $B_\delta(\omega)$ can be employed to evaluate RVE sizes especially if the considered RVE criterion is based not only on the mean value of the apparent behaviors but also on their fluctuations. To this end, the next section is devoted to a statistical study of the apparent properties.

3. A statistical study of the apparent properties of random matrix–fiber composites

As a first illustration, in order to reduce the numerical cost required to compute the apparent behaviors for each realization we consider the case of aligned fiber–matrix composites which can be addressed with low cost 2D simulations.

3.1. Description of the composite

More precisely, the studied material is a two-phase composite made of a matrix and aligned identical non-overlapping fibers randomly and isotropically distributed in the transverse plane. Both phases are isotropic and follow Hooke's law. All results relative to stresses are given in a non-dimensional scale in which the shear modulus of the matrix is $\mu^M = 1$. The contrast c between the phases is such that the bulk and shear moduli are given by $k^I = \mu^I = c$ for the inclusions and $k^M = \mu^M$ for the matrix. It should be noted that the effective behavior of the linear composite is transversally isotropic due to rotational invariance along the fiber axis e_3 of both the behaviors of the constitutive phases and the statistics of their spatial distribution. Further, the same property holds true for the upper and lower bounds $C_\delta^{VOR+/-}$ defined in Eq. (5) (see [18] for detailed explanations). In order to reduce the numerical cost, we only consider the transverse response of the composite. The local problem to be solved can thereby be reduced to a two-dimensional problem in plane strain framework for which the fibers are represented by disks of same diameter d and the VEs are subjected to in-plane loadings.

3.2. Microstructure and non-square VEs generation

The microstructure of the composite is generated by a slightly modified version of the well-known random sequential adsorption (RSA) algorithm [25]. The centers of the disks are randomly and sequentially implemented by a Poisson process in a large window of size $125d$ containing approximatively 3000 fibers for $f = 15\%$. A constraint on the minimum distance between the disks of same diameter d is imposed to prevent overlapping and contact. If the current disk the position of which is randomly chosen in the large window does not satisfy the minimum distance requirement, it is rejected and a new one is generated until the distance condition is fulfilled. New disks are added until the prescribed porosity is reached.

Once a large microstructure is generated, a Voronoï subdivision into elementary cells is performed by using a Matlab function. As explained in Section 2.1, each cell is composed of a sole inclusion surrounded by matrix. Then, n square windows of same size $L = \delta d$ are extracted sequentially from this subdivision by means of a Poisson process providing the centers of the square windows. They are used to generate their corresponding n non-square VEs made of the set of elementary Voronoï cells the centers of which belong to a same δ-sized window. In order to prevent windows overlapping and possible statistical bias, a minimum distance of $\sqrt{2}\delta d$ between the window centers is imposed. Centers are also placed sufficiently far away from the borders of the large microstructure. In order to generate large numbers of VEs, several large microstructures might need to be generated. Details of this procedure are given in [18].

3.3. Computation of the apparent behaviors

Once the generation of the non-square VEs is completed, their apparent stiffness $C^d_\delta(\omega)$ and compliance $S^t_\delta(\omega)$ tensors are computed. For that, the following 2D local problem has been solved in plane strain framework by means of finite element techniques

$$\left\{\begin{array}{l} \left.\begin{array}{l} \operatorname{div}\big(\sigma(x,\omega)\big) = 0 \\ \sigma_m(x,\omega) = 2K(x,\omega)\varepsilon_m(x,\omega), \quad \sigma^d(x,\omega) = 2\mu(x,\omega)\varepsilon^d(x,\omega) \\ \varepsilon(x,\omega) = \dfrac{1}{2}\big(\nabla u(x,\omega) + {}^T\nabla u(x,\omega)\big) \end{array}\right\} \quad \forall x \in \Omega_\delta(\omega) \\ \left.\begin{array}{l} \text{for ADBC:} \quad u(x,\omega) = \bar{\varepsilon}.x \\ \text{for UTBC:} \quad \sigma(x,\omega).n(x,\omega) = \bar{\sigma}.n(x,\omega) \end{array}\right\} \quad \forall x \in \partial\Omega_\delta(\omega) \end{array}\right. \tag{7}$$

where

$$K(x,\omega) = \sum_{r=I,M} K^r \chi^r(x,\omega), \quad K^r = k^r + \mu^r/3, \quad \mu(x,\omega) = \sum_{r=I,M} \mu^r \chi^r(x,\omega) \tag{8}$$

The scalar K^r in Eq. (8) is the in-plane bulk modulus of phase r. In system (7), the decomposition of any second-order tensor field a in plane strain framework into hydrostatic a_m, pure shear a_{ps}, simple shear a_{ss} and deviatoric a^d components has been used:

$$a = a_m i + a_{ps} e_{ps} + a_{ss} e_{ss} = a_m i + a^d \tag{9}$$

where the second-order tensors i, e_{ps} and e_{ss} are defined on the considered Cartesian basis by

$$i = e_1 \otimes e_1 + e_2 \otimes e_2, \qquad e_{ps} = e_1 \otimes e_1 - e_2 \otimes e_2, \qquad e_{ss} = e_1 \otimes e_2 + e_2 \otimes e_1 \tag{10}$$

The in-plane macroscopic strain $\bar{\varepsilon}$ and stress $\bar{\sigma}$ also take the form of Eq. (9).

Although the fibers are isotropically distributed in the transverse plane for the whole microstructure $B(\omega)$, the fibers distribution and as a consequence each ω-realization of the apparent behavior $C^d_\delta(\omega)$, $S^t_\delta(\omega)$ are no longer transversally isotropic for VEs $B_\delta(\omega)$ of finite size δ smaller than the RVE size. In plane strain conditions, the apparent tensors read

$$\begin{aligned} C^d_\delta(\omega) &= 2k^d_\delta(\omega) J_T + 2\lambda^d_\delta(\omega) E_{ps} + 2\mu^d_\delta(\omega) E_{ss} + 2\alpha^d_\delta(\omega) E^s_{m,ps} + 2\beta^d_\delta(\omega) E^s_{m,ss} + 2\gamma^d_\delta(\omega) E^s_{ps,ss} \\ S^t_\delta(\omega) &= \frac{1}{2k^t_\delta(\omega)} J_T + \frac{1}{2\lambda^t_\delta(\omega)} E_{ps} + \frac{1}{2\mu^t_\delta(\omega)} E_{ss} + \frac{1}{2\alpha^t_\delta(\omega)} E^s_{m,ps} + \frac{1}{2\beta^t_\delta(\omega)} E^s_{m,ss} + \frac{1}{2\gamma^t_\delta(\omega)} E^s_{ps,ss} \end{aligned} \tag{11}$$

where the fourth-order tensors J_T, E_{ps}, E_{ss}, $E^s_{m,ps}$, $E^s_{m,ss}$, $E^s_{ps,ss}$ are defined by

$$\begin{aligned} &J_T = \frac{1}{2} i \otimes i, \qquad E_{ps} = \frac{1}{2} e_{ps} \otimes e_{ps}, \qquad E_{ss} = \frac{1}{2} e_{ss} \otimes e_{ss}, \qquad E^s_{m,ps} = \frac{1}{2}(i \otimes e_{ps} + e_{ps} \otimes i) \\ &E^s_{m,ss} = \frac{1}{2}(i \otimes e_{ss} + e_{ss} \otimes i), \qquad E^s_{ps,ss} = \frac{1}{2}(e_{ps} \otimes e_{ss} + e_{ss} \otimes e_{ps}) \end{aligned} \tag{12}$$

The tensors J_T, E_{ps}, E_{ss} (the two latter being recently introduced by Willot et al. [26]) are projectors on the subspaces of isotropic or deviatoric second-order tensors spanned by i, e_{ps}, e_{ss}, respectively. The remaining tensors $E^s_{m,ps}$, $E^s_{m,ss}$, $E^s_{ps,ss}$ — which allow for the coupling between hydrostatic, pure shear and simple shear components — are introduced to fully characterize any material anisotropy in plane strain conditions. The components $k^{d,t}_\delta(\omega)$ are the in-plane apparent bulk modulus for ADBC (d) or UTBC (t) while $\lambda^{d,t}_\delta(\omega)$, $\mu^{d,t}_\delta(\omega)$ are the in-plane apparent pure shear and simple shear moduli, respectively.

The 6 components of the apparent moduli tensor $C^d_\delta(\omega)$ (resp. apparent compliance $S^t_\delta(\omega)$) are classically derived by solving the local problem (7) for 3 different ADBC (resp. UTBC) — e.g. $\bar{\varepsilon} = i$, $\bar{\varepsilon} = e_{ps}$ and $\bar{\varepsilon} = e_{ss}$, thus providing the wanted quantities by averaging the local stress (resp. the local strain) over the whole VE $B_\delta(\omega)$ for each loading.

3.4. Quantities under consideration

The random variables $Z_\delta(\omega)$ on which the statistical study relies are the following:

$$\text{for ADBC:}\quad Z_\delta^d(\omega) = \underbrace{K_\delta^d(\omega), G_\delta^d(\omega)}_{\text{isotropic part}}, \underbrace{\frac{\mu_\delta^d(\omega)-\lambda_\delta^d(\omega)}{2}, \alpha_\delta^d(\omega), \beta_\delta^d(\omega), \gamma_\delta^d(\omega)}_{\text{deviation from isotropy}}$$

$$\text{for UTBC:}\quad Z_\delta^t(\omega) = \overbrace{\frac{1}{K_\delta^t(\omega)}, \frac{1}{G_\delta^t(\omega)}}, \overbrace{\frac{1}{2}\left(\frac{1}{\mu_\delta^t(\omega)}-\frac{1}{\lambda_\delta^t(\omega)}\right), \frac{1}{\alpha_\delta^t(\omega)}, \frac{1}{\beta_\delta^t(\omega)}, \frac{1}{\gamma_\delta^t(\omega)}} \tag{13}$$

In relation (13), the moduli $K_\delta^d(\omega), K_\delta^t(\omega), G_\delta^d(\omega), G_\delta^t(\omega)$ defined by

$$K_\delta^d(\omega) = \frac{C_\delta^d(\omega) : J_T}{2}, \qquad G_\delta^d(\omega) = \frac{C_\delta^d(\omega) : K_T}{4}, \qquad \frac{1}{K_\delta^t(\omega)} = \frac{S_\delta^t(\omega) : J_T}{2}, \qquad \frac{1}{G_\delta^t(\omega)} = \frac{S_\delta^t(\omega) : K_T}{4} \tag{14}$$

are the 2D-isotropic projections of the apparent moduli $C_\delta^d(\omega)$ and compliance $S_\delta^t(\omega)$ tensors where $K_T = E_{ps} + E_{ss}$ is the usual projector on the subspace of purely in-plane deviatoric second-order tensors. They satisfy the following relations:

$$K_\delta^d(\omega) = k_\delta^d(\omega), \qquad G_\delta^d(\omega) = \frac{\lambda_\delta^d(\omega)+\mu_\delta^d(\omega)}{2}, \qquad K_\delta^t(\omega) = k_\delta^t(\omega), \qquad G_\delta^t(\omega) = 2\left(\frac{1}{\mu_\delta^t(\omega)}+\frac{1}{\lambda_\delta^t(\omega)}\right)^{-1} \tag{15}$$

Accordingly, as seen in formula (13), the random variables $Z_\delta(\omega)$ can be classified into two parts. The first part consists of random variables characterizing the isotropic part of the apparent moduli $C_\delta^d(\omega)$ and compliance $S_\delta^t(\omega)$, namely $K_\delta^d(\omega)$, $G_\delta^d(\omega)$, $K_\delta^t(\omega)$ and $G_\delta^t(\omega)$. The second part is made of the components of the moduli or compliance tensors which characterize their deviation from isotropy, i.e. $(\mu_\delta^d(\omega)-\lambda_\delta^d(\omega))/2$, $\alpha_\delta^d(\omega)$, $\beta_\delta^d(\omega)$, $\gamma_\delta^d(\omega)$, $(1/\mu_\delta^t(\omega)-1/\lambda_\delta^t(\omega))/2$, $1/\alpha_\delta^t(\omega)$, $1/\beta_\delta^t(\omega)$, $1/\gamma_\delta^t(\omega)$.

It should be noted that the computation of the VOR bounds of the effective properties only makes use of the moduli $Z_\delta(\omega)$ characterizing the isotropic part of the apparent behaviors. Indeed, as explained in Section 3.1, both the effective behavior C^{eff} and Voronoï bounds $C_\delta^{VOR+/-}$ are transversally isotropic due to the rotational invariance along the fiber axis.[1] Accordingly, in plane strain framework, they are written

$$C^{eff} = 2K^{eff}J_T + 2G^{eff}K_T, \qquad C_\delta^{VOR+/-} = 2K_\delta^{VOR+/-}J_T + 2G_\delta^{VOR+/-}K_T \tag{16}$$

where K and G denote the in-plane bulk and shear moduli. Applying Eq. (16) to inequalities (6) yields

$$K_\delta^{VOR-} \leqslant K^{eff} \leqslant K_\delta^{VOR+}, \qquad G_\delta^{VOR-} \leqslant G^{eff} \leqslant G_\delta^{VOR+} \tag{17}$$

where the VOR bounds for transversally isotropic behaviors can be estimated by the following relations:

$$K_\delta^{VOR+} = E\big(K_\delta^d\big), \qquad K_\delta^{VOR-} = \left(E\left(\frac{1}{K_\delta^t}\right)\right)^{-1}, \qquad G_\delta^{VOR+} = E\big(\lambda_\delta^d\big) = E\big(\mu_\delta^d\big) = E\big(G_\delta^d\big)$$
$$G_\delta^{VOR-} = \left(E\left(\frac{1}{\lambda_\delta^t}\right)\right)^{-1} = \left(E\left(\frac{1}{\mu_\delta^t}\right)\right)^{-1} = \left(E\left(\frac{1}{G_\delta^t}\right)\right)^{-1} \tag{18}$$

Formulae (18) are straightforwardly derived by making use of both the transverse isotropy and definitions (5) of the VOR bounds.

The statistical study aims at analyzing the fluctuations of the above-mentioned random variables $Z_\delta(\omega)$. They depend on several parameters such as the considered mechanical property — namely the moduli $Z_\delta(\omega)$ itself, the BC, the fluctuations of the microstructure which in the following will be referred to as the individual fluctuations, the size δ of the VE, the contrast between the phases and lastly the inclusion volume fraction. In this work, the analysis of the fluctuations of any random variable $Z_\delta(\omega)$ is performed by means of both its coefficient of variation $CoV(Z_\delta) = \sigma(Z_\delta)/E(Z_\delta)$, which only provides partial information about the statistic of $Z_\delta(\omega)$, and its probability density function $pdf(Z_\delta)$ which contains the whole statistics of $Z_\delta(\omega)$. Remember that the pdf of $Z_\delta(\omega)$ is computed by ascribing to each w-realization of $Z_\delta(\omega)$ its weight $V_\delta(\omega)/E(V_\delta)$. In order to quantify the influence of the BC on the moduli fluctuations, we also compute the fluctuations $\Delta Z_\delta^{VOR}/Z_\delta^{VOR}$ referred in the following to as the moduli BC-based fluctuations and defined as follows:

[1] Rigorously speaking, the VOR bounds still depend on the geometry of the square domains Ω_δ^s by which the Voronoï cells are selected to define the VEs. Therefore, they may keep some kind of quadratic symmetry. But in practice, this anisotropy is so small that it can be neglected.

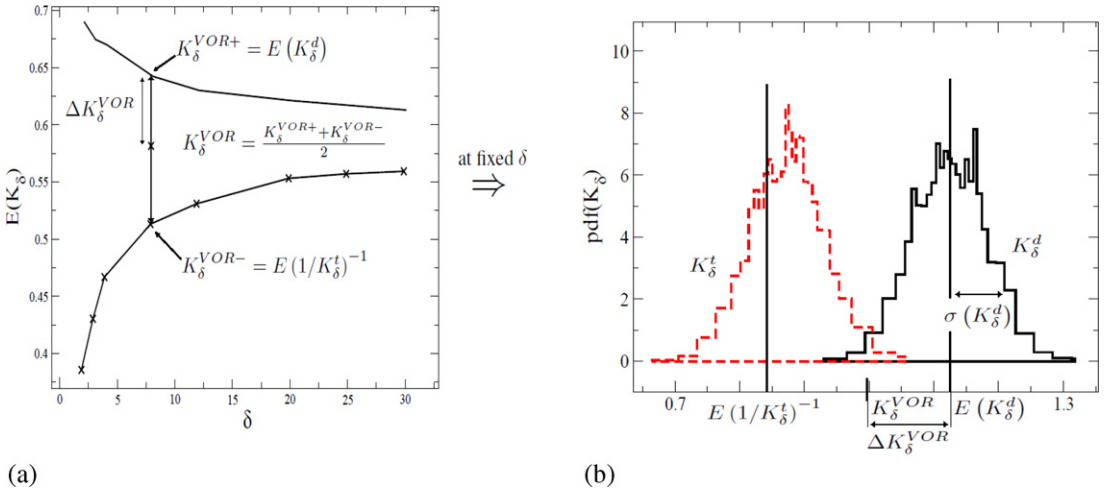

Fig. 2. Graphical interpretation of the fluctuations $\Delta K_\delta^{VOR}/K_\delta^{VOR}$ (a) and $CoV(K_\delta^d) = \sigma(K_\delta^d)/E(K_\delta^d)$ (b) of the apparent bulk modulus.

$$\frac{\Delta Z_\delta^{VOR}}{Z_\delta^{VOR}} = \frac{Z_\delta^{VOR+} - Z_\delta^{VOR-}}{Z_\delta^{VOR+} + Z_\delta^{VOR-}} = \frac{E(Z_\delta^d) - E(1/Z_\delta^t)^{-1}}{E(Z_\delta^d) + E(1/Z_\delta^t)^{-1}} \tag{19}$$

for $Z_\delta(\omega) = K_\delta^{d,t}(\omega), G_\delta^{d,t}(\omega)$. According to definition (19), the effects of the individual fluctuations of the microstructure are not taken into account by the quantity $\Delta Z_\delta^{VOR}/Z_\delta^{VOR}$. Indeed, by performing ensemble averaging on the random variables the quantity $\Delta Z_\delta^{VOR}/Z_\delta^{VOR}$ only incorporates the BC effects on the moduli fluctuations unlike the CoV fluctuations which do depend on the individual fluctuations of the microstructure as well as on the BC. As an illustration, Fig. 2 provides a graphical interpretation of both fluctuations $\Delta K_\delta^{VOR}/K_\delta^{VOR}$ and $CV(K_\delta^d)$ of the apparent in-plane bulk moduli — note that $E(1/K_\delta^t)^{-1}$ is not the mean value of K_δ^t.

Lastly, we define and compute the following quantities:

$$\begin{aligned}
\Delta_{iso}^d &= \sqrt{E\left(\left(\frac{\mu_\delta^d - \lambda_\delta^d}{2}\right)^2 + \left(\alpha_\delta^d\right)^2 + \left(\beta_\delta^d\right)^2 + \left(\gamma_\delta^d\right)^2\right)} \\
\Delta_{iso}^t &= \sqrt{E\left(\left(\frac{1}{2}\left(\frac{1}{\mu_\delta^t} - \frac{1}{\lambda_\delta^t}\right)\right)^2 + \left(\frac{1}{\alpha_\delta^t}\right)^2 + \left(\frac{1}{\beta_\delta^t}\right)^2 + \left(\frac{1}{\gamma_\delta^t}\right)^2\right)}
\end{aligned} \tag{20}$$

which can be interpreted as statistical measures of the deviation from isotropy of the apparent behavior. Such measures can provide interesting information about the RVE size. Indeed, as seen in Section 3.1 the effective behavior of the considered composite is transversally isotropic. Accordingly, the convergence with respect to δ of these measures towards zero — at a given accuracy — can be used for instance as a necessary condition which should be satisfied for a minimum RVE size.

3.5. Results

All numerical applications of this work have been carried out for both a rigidly reinforced composite ($c = 10^4$) and a porous material ($c = 10^{-4}$) and for two inclusion volume fractions ($f^I = 15\%, 30\%$). In a few cases, computations have also been run for other contrasts ranging from 10^{-2} to 10^2. For all numerical applications, the number of realizations n is set to $n = 2000$ for $2 \leqslant \delta < 20$ or $n = 1000$ for $20 \leqslant \delta \leqslant 30$.

3.5.1. Relative fluctuations induced by the variability of the microstructure and BC

Figs. 3 and 4 depict in logarithmic scales the variations with respect to δ of the CoV of the apparent in-plane bulk (a) and shear (b) moduli for the reinforced composite and the porous material, respectively, and for both volume fractions ($f^I = 15\%, 30\%$). First, it is noted that, as expected, the fluctuations of the apparent in-plane bulk and shear moduli of both the reinforced composite and porous material regularly decrease and tend towards zero when δ is increasing. Qualitatively speaking, the rate of this decrease is similar for both moduli and both composites. However, the fluctuation levels for a given VE size δ are larger in the porous material than in the reinforced composite; this is especially true for the in-plane shear modulus, which exhibits CoVs up to 5 times larger in the porous material. This suggests that the RVE size would be larger for the porous material than for the rigidly reinforced composite, at least for the shear modulus. Second, it is also observed that the fluctuations of both the apparent in-plane bulk and shear moduli have the same order of magnitude for the rigidly reinforced composite while for the porous material the fluctuations of the in-plane shear modulus are larger than those of

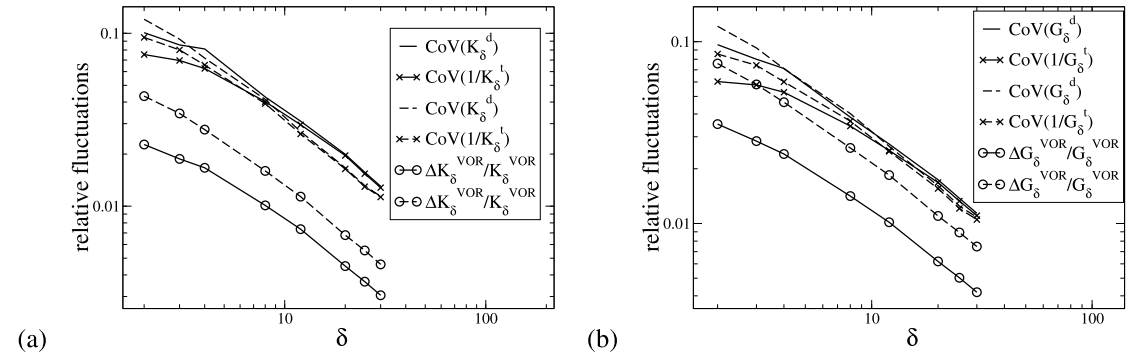

Fig. 3. Rigidly reinforced composite ($c = 10^4$): variations as a function of δ of the CoV and BC-based fluctuations for the apparent in-plane bulk (a) and shear (b) moduli or compliances computed either with ADBC or UTBC. Continuous lines are relative to $f^I = 15\%$ while dashed curves are related to $f^I = 30\%$.

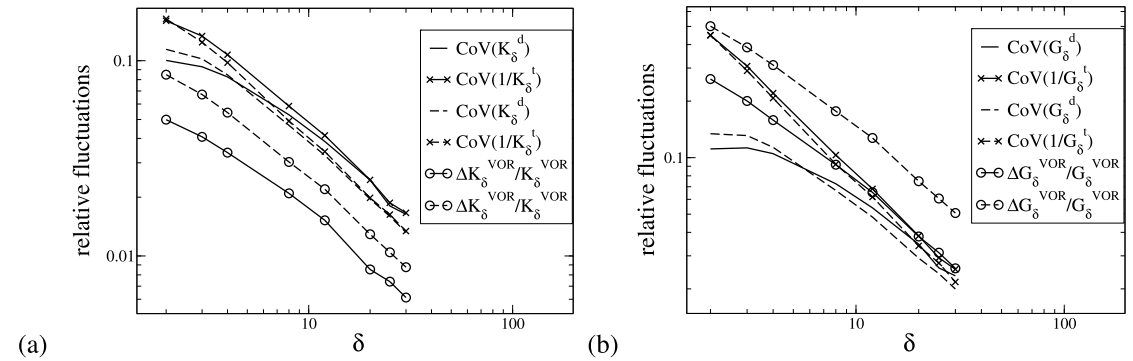

Fig. 4. Porous material ($c = 10^{-4}$): variations as a function of δ of the CoV and BC-based fluctuations for the apparent in-plane bulk (a) and shear (b) moduli or compliances computed either with ADBC or UTBC. Continuous lines are relative to $f^I = 15\%$ while dashed curves are related to $f^I = 30\%$.

the in-plane bulk modulus. This trend suggests that the RVE size associated with the shear modulus would be larger than the one associated with the bulk modulus for the porous material. Third, the discrepancy between the CoV associated with ADBC and UTBC converges more quickly to zero than the CoVs themselves, thus showing that the influence of the BC on the moduli fluctuations is of shorter range than the individual fluctuations one. More precisely, this remark holds true for all situations depicted in Figs. 3 and 4 except for the in-plane shear modulus of the porous material (Fig. 4(b)). This trend is corroborated by the evolutions with respect to δ of the BC-based fluctuations $\Delta Z_\delta^{VOR}/Z_\delta^{VOR}$ of the apparent in-plane bulk and shear moduli which are also reported in Figs. 3 and 4. Indeed, except again for Fig. 4(b), the BC-based fluctuations are notably lower than the CoVs and are almost negligible from a value δ which approximatively corresponds to the value for which both CoVs associated respectively with ADBC and UTBC tend to merge. This seems to confirm the fact that the effect of individual fluctuations of the microstructure on the moduli fluctuations has a larger range than the one induced by the BC, of course to the notable exception of the apparent shear moduli fluctuations for the porous material. Indeed, in this case both effects are of similar intensity for low volume fraction and the influence of BC notably exceeds that of the individual fluctuations of microstructure for higher volume fraction. Lastly, it is noted that the moduli fluctuations of a rigidly reinforced composite for small δ are more pronounced when associated with ADBC than with UTBC. The converse is observed for porous materials.

Concerning the influence of the inclusion or pore volume fraction, we first notice a pronounced increase of the BC-based fluctuations for both moduli and both the rigidly reinforced composite and the porous material when f^I is increased from 15 to 30%. This can easily be explained by the fact that the inclusions get on average closer to the boundaries of the cells and are thus more sensitive to the boundary conditions. For very low volume fractions, inclusions would be far away from each other and from cell boundaries so that most of them would behave as Eshelby's [27] heterogeneous inclusion. Both VOR bounds would then converge to the dilute estimate for cylindrical inclusions and the BC-based fluctuations are expected to vanish. With increasing volume fraction, interaction terms get more and more important and the gap between ADBC or UTBC bounds, for a given window size, is expected to grow, as observed. The second observed effect is a slight decrease with volume fraction of the CoV for large δ and a small increase for small δ, for both moduli of the reinforced composite. Similar trends are observed for both apparent moduli of the porous material associated with ADBC while a slight decrease for all δ is observed for the apparent properties associated with UTBC. This more complex behavior is less easy to explain. It is the consequence of the combination of several effects with potentially opposite tendencies. The first one is linked to the variability of the local configurations of the microstructure, which can be higher for low and intermediate δ

than for higher δ, near the packing limit of the RSA algorithm, for which the relative positions of the inclusions are much more constrained by the non-overlapping condition. In particular, the volume fractions of the VOR windows are likely to be closer to the prescribed overall volume fraction when the latter is high and when δ is large, while they are expected to fluctuate much more for small overall volume fractions and small δ. The second effect is linked to the mechanical interactions between inclusions and between inclusions and boundaries. They are clearly very limited for small volume fractions for which most inclusions would behave as Eshelby's isolated one, as already mentioned above. However a few of them could still be close to boundaries and sensitive to the applied loads, and contribute to an increase of the CoV, even if their contribution to the ensemble averages leading to the VOR bounds might be very small. The contributions of these marginal configurations are likely to be larger for small δ. For higher volume fractions, interaction effects are clearly more important, and may contribute to a larger variability of the apparent behavior. But for high volume fractions and sufficiently large windows, the variability of these interaction effects will be limited because of the already mentioned limited variability of the microstructure itself. The combination of these effects leads to complex evolutions of the CoVs with volume fractions, which might be non-monotonous and exhibit local maxima for some critical volume fractions. Before this maximum, variability of microstructure and increasing interaction effects tend to increase the fluctuations of the apparent behavior, while above it, the reduction of the variability of the microstructure would overcome interaction effects. The detailed quantitative analysis of such evolutions would however require more numerical simulations, which are left for further investigations.

Lastly, as can be seen in Figs. 3 and 4, the evolutions of the CoVs with respect to δ follow for large enough values of δ a scaling function given by $\log(CoV(Z_\delta^{d,t})) = a\log\delta + \log(b^{d,t}(Z))$ where $a \simeq -1$ and $b^{d,t}(Z)$ is a constant which depends on both the applied BC and the considered material property Z. Numerical applications carried out for other contrasts ranging from 10^{-2} to 10^2 show that this scaling function — which can be rewritten as $CoV(Z_\delta^{d,t})\delta = b^{d,t}(Z)$ — works not only for infinite contrasts but also for every contrast. For lower δ, the slopes of the curves are lower. The critical δ above which the -1 slope is observed seems to coincide again with the size at which the CoVs associated with ADBC and UTBC tend to merge. Note that such an evolution of CoVs proportional to $1/\delta$ would be observed if the computation of apparent properties of a VE of size δ would be equivalent to four independent computations on VEs of size $\delta/2$. See also Willot and Jeulin [28] for the theoretical justification of such an asymptotic behavior based on the concept of integral range of the local fields. This transition seems thus to coincide with some disappearance of the influence of BC on the apparent behavior. The size δ at which that occurs depends on the contrast and, to some lower extend, the volume fraction. It is for instance close to $\delta = 20$ in Fig. 3(a).

3.5.2. Probability density function

Fig. 5 reports the probability density functions of the apparent in-plane bulk moduli $K_\delta^{d/t}(\omega)$ of the rigidly reinforced composite for two values of both the VE size ($\delta = 2, \delta = 12$) and the inclusion volume fraction ($f^I = 15\%$, $f^I = 30\%$). For comparison purposes, Gaussian distributions with mean $E(K_\delta^d)$ and standard deviation $\sigma(K_\delta^d)$ are also depicted in Fig. 5 for the same values of δ and f^I. The same curves are reported in Fig. 6 for the apparent in-plane shear moduli $G_\delta^{d/t}(\omega)$ for the porous material. In both Figs. 5 and 6, all apparent bulk or shear moduli are normalized by their corresponding effective moduli which are estimated by

$$K^{eff} = \frac{E(K^d_{\delta=30}) + E(K^t_{\delta=30})}{2}, \qquad G^{eff} = \frac{E(G^d_{\delta=30}) + E(G^t_{\delta=30})}{2} \tag{21}$$

As shown in Fig. 5(a), the pdfs of both apparent in-plane bulk moduli $K_\delta^{d/t}(\omega)$ are rather close to each other, even though, as expected from the bounding properties (6), the pdf of $K_\delta^d(\omega)$ is slightly shifted to the right. Both pdfs are right-skewed with a rather long upper tail and no lower tail. It is noted that the VEs $B_\delta(\omega)$ at $\delta = 2$ mainly consist of a single Voronoï cell even though there is also in a sizeable quantity some VEs made of the concatenation of two Voronoï cells. For such two-cell-type VEs, it is noted that their local inclusion volume fractions are usually larger than the global one, i.e. f^I, thus inducing stiffer apparent moduli for reinforced composites than their mean value $E(K_\delta^{d/t})$. This explains the shape of the $K_\delta^d(\omega)$ or $K_\delta^t(\omega)$ pdfs where the apparent moduli associated with these two-cell-type VEs contribute to the upper tail of the distribution while the ones related to one-cell-type VEs compose the mass of the distribution. The shape of the $K_\delta^{d/t}(\omega)$ distributions slightly evolves with respect to δ and attains a Gaussian shape from $\delta = 12$, as can be seen in Fig. 5(b) where both the Gaussian distribution (with mean $E(K_\delta^d)$ and standard deviation $\sigma(K_\delta^d)$) and the pdf of $K_\delta^d(\omega)$ nearly coincide. From $\delta = 12$, the pdfs keep their Gaussian shape when δ is increasing and as expected their mean values converge towards the effective bulk modulus while their standard deviation tends to zero.

For a larger inclusion volume fraction $f^I = 30\%$, the evolutions of the $K_\delta^{d/t}(\omega)$ pdfs as functions of δ are the same as for $f^I = 15\%$ (see Fig. 5(d)) except for small values of δ. Indeed, as shown in Fig. 5(c), at $\delta = 2$ the $K_\delta^{d/t}(\omega)$ pdfs are already close to a Gaussian distribution albeit they are still a little right-skewed. The new shape of the distribution is due to the fact that for $f^I = 30\%$ most VEs are now composed of two Voronoï cells while a sizeable number of VEs are composed of one or three even four Voronoï cells. For one-cell-type VEs, the local inclusion volume fractions are most of the time smaller than f^I thus inducing softer apparent moduli than the mean of the whole apparent behavior while the opposite trends occur for three- or four-cell-type VEs. The one-cell-type VEs and the two-cell-type VEs provide the lower tail and the mass of the distribution, respectively, while the three- or four-cell-type VEs yield the upper tail. This explains why, for small values of δ,

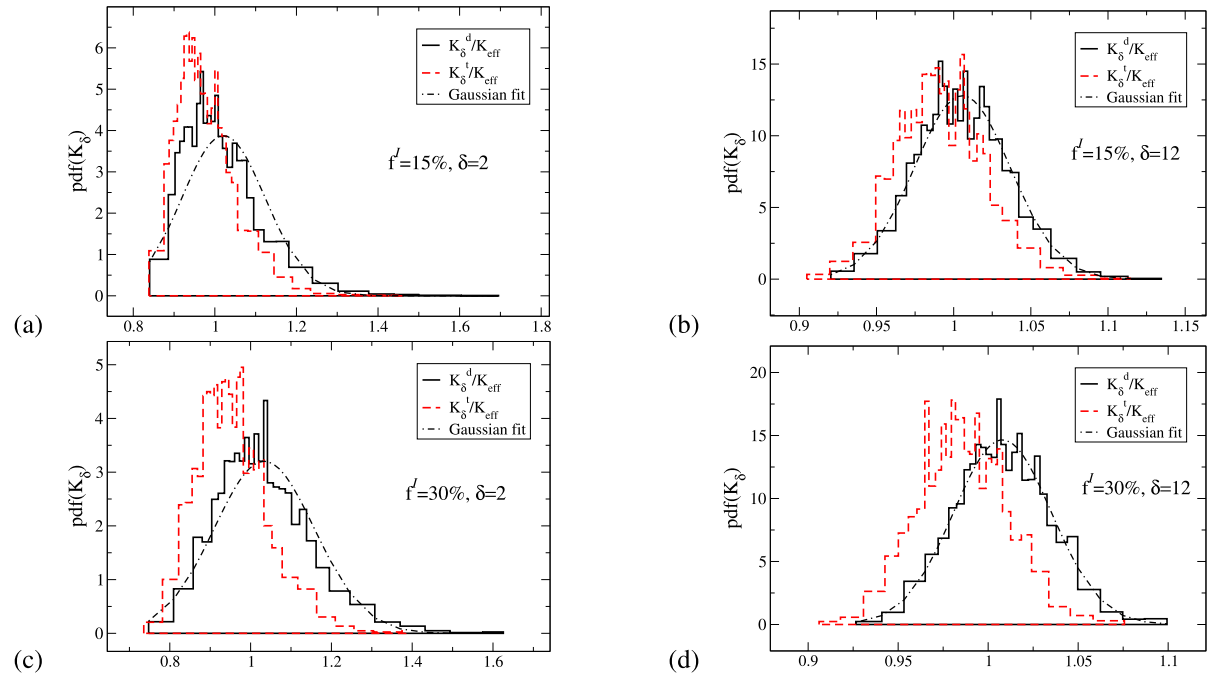

Fig. 5. Rigidly reinforced composite ($c = 10^4$). Probability density functions of the normalized apparent in-plane bulk moduli K_δ^d/K^{eff}, K_δ^t/K^{eff} and of the Gaussian distribution associated with K_δ^d/K^{eff} for various values of f^I and δ.

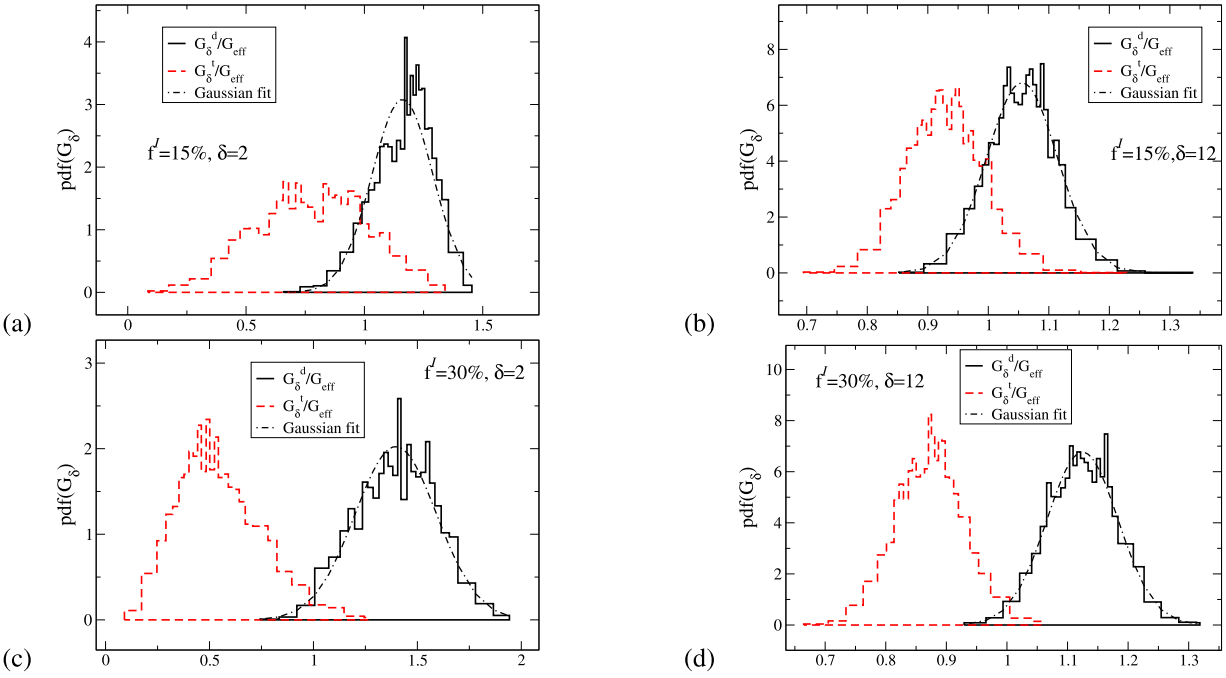

Fig. 6. Porous material ($c = 10^{-4}$). Probability density functions of the normalized apparent in-plane shear moduli G_δ^d/G^{eff}, G_δ^t/G^{eff} and of the Gaussian distribution associated with G_δ^d/G^{eff} for various values of f^I and δ.

the $K_\delta^{d/t}(\omega)$ pdfs are more symmetric and close to a Gaussian distribution for higher volume fractions than for smaller ones. The same trends as the ones observed in Fig. 5 are found again for the shear moduli pdf of rigidly reinforced materials.

For porous materials, as illustrated in Fig. 6 for the shear modulus, the trends are also similar to the ones observed in Fig. 5 except that now the shift between the pdfs respectively associated with ADBC or UTBC is much more pronounced than the one observed for rigidly reinforced composites, consistently with results of Fig. 4.

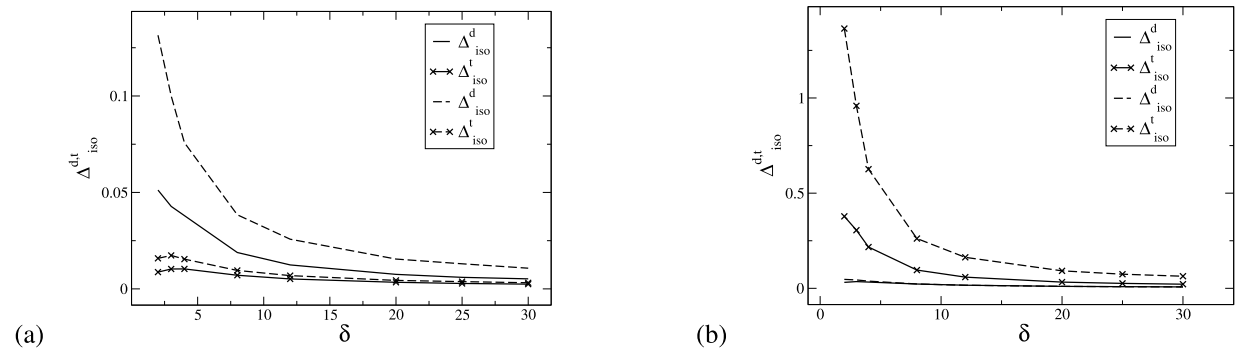

Fig. 7. Variations of the statistical measures of the deviation from isotropy $\Delta^{d/t}_{iso}$ as functions of δ for a rigidly reinforced composite (a) and a porous material (b). Continuous lines are relative to $f^I = 15\%$ while dashed curves are related to $f^I = 30\%$.

3.5.3. Deviation from isotropy

The evolutions with respect to δ of the statistical measures $\Delta^{d/t}_{iso}$ — defined in Eq. (20) — of the deviation from isotropy of the apparent behavior are reported for the rigidly reinforced composite and the porous material in Figs. 7(a) and 7(b), respectively. They are computed for two inclusion or pore volume fractions ($f^I = 15\%$, $f^I = 30\%$). For the reinforced composite, as shown in Fig. 7(a), both global measures of the deviation from isotropy quickly converge to zero for both volume fractions. This implies that almost all individual ω-realizations of the apparent moduli $C^{d/t}_{\delta}(\omega)$ are isotropic for a relatively small value of the VE size. The same trends are observed for the porous material in Fig. 7(b) albeit the anisotropy of the individual realization is significantly more pronounced than for the rigidly reinforced composite — i.e. $\Delta^{d/t}_{iso}$ are larger for porous materials than for rigidly reinforced ones. Accordingly, in agreement with the whole results obtained in the previous sections, the influences of both the BC and individual fluctuations of the microstructure as well as the anisotropy of the VEs $B_{\delta}(\omega)$ on the apparent behavior are stronger for the porous material than for the rigidly reinforced composites. It is also observed that the apparent behaviors of both the rigidly reinforced composite and the porous material are closer to an isotropic behavior for $f = 15\%$ than for $f = 30\%$. This can be explained by the fact that anisotropy is only induced by the interaction effects between fibers or pores, which are more pronounced at higher volume fractions. Lastly, note that the apparent behaviors based on UTBC are significantly more anisotropic than those based on ADBC for porous materials while the converse holds true for reinforced composites.

4. RVE size

In this section, we present some proposals of RVE criteria based both on the numerical approach introduced in Section 2 and on the fluctuations of the apparent moduli which have been studied in Section 3. For that, we consider two different ways to define an RVE from a qualitative viewpoint. Inside each of both these RVE categories we then propose RVE criteria providing quantitative definitions of the RVE size. For the first RVE type, the RVE size is defined as the minimum size required to evaluate at some accuracy the effective property from apparent properties of VEs of size δ. In the following, this type of RVE will be referred to as "computational RVE" since all the criteria mentioned in the introduction and belonging to this type of RVE [19,11,3,10,13,17] make use of computational schemes to determine the effective behavior, and are focused on the development of methodologies to compute effective properties, without considerations on the conditions which allow to describe heterogeneous materials with equivalent homogeneous ones. The second viewpoint defines the RVE as the smallest VE inside which the heterogeneous material can be replaced by a homogeneous equivalent one having the effective properties in a given structural mechanics problem, without considering statistical expectations over possible realization of the material microstructure. Implicitly, this second RVE type requires that nearly all realizations of an RVE $B_{\delta_{RVE}}(\omega)$ should provide an accurate estimate of the effective behavior, and is thus more demanding than the first one for which only ensemble averages are expected to be close to the effective behavior. In the sequel, the second type of RVE will be referred to as "equivalent medium-based RVE".

4.1. Computational RVE based on the independence w.r.t. BC

Recalling the bound status of $Z^{VOR+/-}_{\delta}$ for a modulus Z corresponding either to the in-plane bulk K or shear G modulus, a very simple RVE criterion can be obtained by considering that the RVE size related to a property Z is reached for a given accuracy ε when the BC-based fluctuations $\Delta Z^{VOR}_{\delta}/Z^{VOR}_{\delta}$ defined by Eq. (19) satisfy $\Delta Z^{VOR}_{\delta}/Z^{VOR}_{\delta} \leqslant \varepsilon$. As already noticed in Section 3.4, $\Delta Z^{VOR}_{\delta}/Z^{VOR}_{\delta}$ and therefore the RVE criterion are only based on the independence of the effective behavior with respect to the BC since the effects of the individual fluctuations of the microstructure are removed when performing ensemble weighted averages of the apparent properties $Z^{d/t}_{\delta}(\omega)$ on which relies the definition of $\Delta Z^{VOR}_{\delta}/Z^{VOR}_{\delta}$. However, such a definition of the RVE size is too approximative since it gives no information about the accuracy used to compute the

required ensemble averages and therefore should be slightly modified by making use of the confidence interval (CI) notion. For a scalar random variable $X(\omega)$, the $(1-\alpha)$-confidence interval of its ensemble average $E(X)$ derived from n realizations of X, is given by

$$CI^n_{1-\alpha}\big(E(X)\big) = \left[\overline{X}_n - t(\alpha,n)\frac{S_n}{\sqrt{n}}, \overline{X}_n + t(\alpha,n)\frac{S_n}{\sqrt{n}}\right] \tag{22}$$

with $\overline{X}_n = \frac{1}{n}\sum_{i=1}^n \frac{V_\delta(\omega_i)}{\overline{V}_\delta} X(\omega_i)$, $S_n^2 = \frac{1}{n-1}\sum_{i=1}^n \frac{V_\delta(\omega_i)}{\overline{V}_\delta}(X(\omega_i)-\overline{X}_n)^2$ and where $(X(\omega_i), \omega_i \in \Theta, 1 \leqslant i \leqslant n)$ are the n independent realizations of $X(\omega)$. The parameter $t(\alpha,n)$ is a positive real number provided by the Student distribution tables. For a detailed definition of the CI, see [29]. Since, by definition, the probability that $E(X)$ belongs to this CI is equal to $1-\alpha$, the length $\frac{t(\alpha,n)S_n}{\sqrt{n}}$ is a probabilistic characterization of the relative accuracy of the estimated expectation value $\overline{X}_n$. Starting from Eq. (17), the definition of the confidence interval implies

$$P\big(Z^-_{\delta,est} \leqslant Z^{eff} \leqslant Z^+_{\delta,est}\big) \geqslant 1-\alpha \tag{23}$$

where

$$Z^+_{\delta,est} = \overline{Z^d_\delta} + \ell^{CI}\big(E\big(Z^d_\delta\big)\big), \qquad Z^-_{\delta,est} = \big(\overline{1/Z^t_\delta} + \ell^{CI}\big(1/Z^t_\delta\big)\big)^{-1} \tag{24}$$

for $Z = K$ or G. In Eq. (24), $\ell^{CI}(E(X))$ denotes the half length of the $(1-\alpha)$-confidence interval of $E(X)$, i.e. $\ell^{CI}(E(X)) = \frac{t(\alpha,n)S_n}{\sqrt{n}}$. To simplify the notations in Eq. (24), the dependence on n of $\overline{X}$ and on n and α of both $\ell^{CI}(E(X))$ and $Z^\pm_{\delta,est}$ are omitted.

From Eq. (23), a more relevant definition of the RVE size $\delta_{BC}(Z)$ for a property Z, e.g. the in-plane bulk or shear modulus, at an accuracy ε is given by

$$\delta_{BC}(Z) = \min_\delta\left\{\delta, \frac{\Delta Z^{eff}_\delta}{Z^{eff}_\delta} < \varepsilon\right\} \quad \text{where } Z^{eff}_\delta = \frac{Z^+_{\delta,est} + Z^-_{\delta,est}}{2}, \quad \Delta Z^{eff}_\delta = \frac{Z^+_{\delta,est} - Z^-_{\delta,est}}{2} \tag{25}$$

In terms of probabilistic interpretation, due to relations (23) and (25), the probability for the relative error $\Delta Z^{eff}_\delta / Z^{eff}_\delta$ of the effective property to be smaller than ε is greater than $(1-\alpha)$ for $\delta \geqslant \delta_{BC}$. It should be noted that δ_{BC} does not only depend on the considered property Z but also on both accuracies (ε,α), on the number of realizations n as well as on f^I and c.

In what follows, for all numerical applications, a 0.99-confidence interval (i.e. $\alpha = 0.01$) is used. For such an interval, recalling that $n = 2000$ for $2 \leqslant \delta < 20$ or $n = 1000$ for $20 \leqslant \delta \leqslant 30$, the Student parameter $t(\alpha,n)$ is given by $t(0.01,n) = 2.56$ for all $n \geqslant 100$. Numerical applications have been carried out for 8 values of the contrast ($c = 10^{-4}, 10^{-2}, 10^{-1}, 0.2, 5, 10, 10^2, 10^4$) and two different inclusion volume fractions ($f^I = 15\%, 30\%$). Fig. 8 reports the evolutions of the RVE size δ_{BC} associated with either the bulk effective modulus (Fig. 8(a)) or the shear effective modulus (Fig. 8(b)) as functions of the contrast for 3 different values of the accuracy ($\varepsilon = 1\%, 2\%, 5\%$). In what follows, for the case where the RVE size is still not reached at $\delta = 30$ for a given contrast and accuracy, δ_{BC} is not reported on the plots. Furthermore, when the RVE size is already attained at $\delta = 2$, the value of δ_{BC} which is reported on the plot is set to 2. As can be seen, for a given accuracy ε and inclusion volume fraction f^I, the RVE size associated with the effective shear modulus is always larger than the one associated with the bulk modulus. Furthermore, as expected the maximal values of the RVE size are obtained for infinite contrasts, i.e. for the rigidly reinforced composite ($c = 10^4$) and the porous material ($c = 10^{-4}$). However, the RVE size of the porous material is always larger than the one of the rigidly reinforced composite. Lastly, an increase of the inclusion volume fraction provides an increase of the RVE size which seems to be more significant for fiber-softened composites ($c < 1$) than for reinforced ones ($c > 1$). Similar arguments as those presented in Section 3.5.1 for the moduli fluctuations can be used to provide more insight about the influence of the inclusion volume fraction on the RVE size.

Note finally that the results used to generate plots in Fig. 8 could also be used to specify for a given δ the number n of realizations required to reduce the confidence interval to an expected width, as in [13]. Such a point of view is not detailed for brevity.

4.2. Equivalent medium-based RVE

This section aims at defining a minimum RVE size from which the heterogeneous material can be replaced by a fictitious homogeneous one in structural calculations. Such an operation requires to make use of an RVE for which individual fluctuations of the apparent properties remain small. Two variants of this approach are considered. In the simpler first one, only the individual fluctuations of the apparent properties for both ADBC and UTBC are considered, assuming that the discrepancies between the expectations of these two estimates can be neglected as suggested by results in Figs. 3 and 4(a). For the second one both individual fluctuations and influence of BC are taken into account, in a more rigorous approach taking into account to whole pdfs.

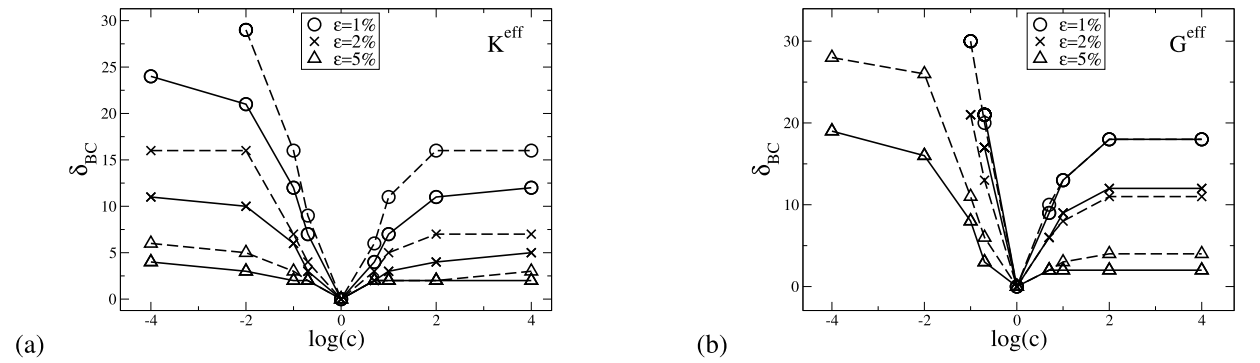

Fig. 8. Variations of the RVE size δ_{BC} associated with the bulk effective modulus (a) or the shear effective modulus (b) with respect to the contrast c for different values of the accuracy ε and the inclusion volume fraction f^I. Continuous lines are relative to $f^I = 15\%$ while dashed curves are related to $f^I = 30\%$.

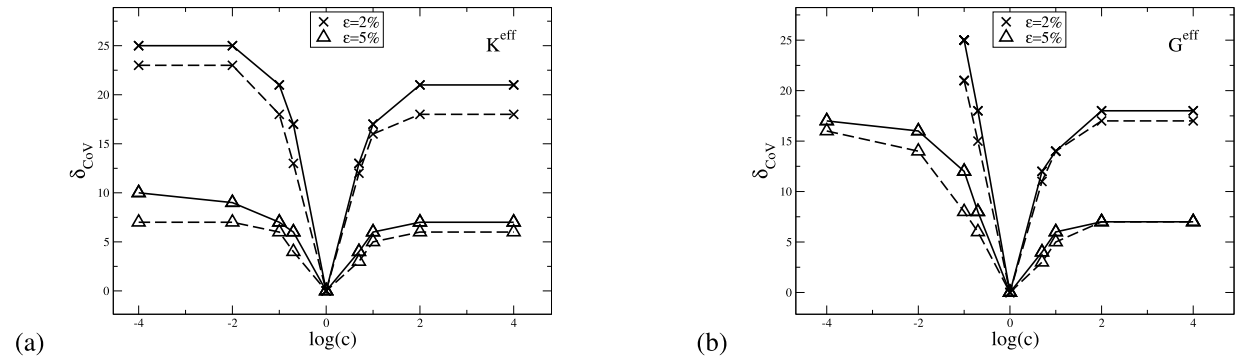

Fig. 9. Variations of the RVE size δ_{CoV} associated with the bulk (a) or shear (b) effective modulus with respect to the contrast c for different values of the accuracy ε and inclusion volume fraction f^I. Continuous lines are relative to $f^I = 15\%$ while dashed curves are related to $f^I = 30\%$.

4.2.1. RVE criterion based on the coefficient of variation

The second proposed RVE criterion has already been used in the literature (e.g. [30]) in combination with other procedures to compute apparent properties. It consists in determining the minimum VE size from which the CoV of a given apparent property $Z_\delta^{d,t}(\omega)$ is smaller than the wanted accuracy ε, namely

$$\delta_{CoV}^{d,t}(Z) = \min_{\delta}\left\{\delta, CoV\left(Z_\delta^{d,t}\right) = \sigma\left(Z_\delta^{d,t}\right)/E\left(Z_\delta^{d,t}\right) < \varepsilon\right\} \tag{26}$$

To define from $\delta_{CoV}^{d/t}(Z)$ an RVE criterion which as expected does not depend on the BC, we simply take the supremum on both BC, i.e. $\delta_{CoV}(Z) = \sup\{\delta_{CoV}^{d}(Z), \delta_{CoV}^{t}(Z)\}$. It should be noted that $\delta_{CoV}(Z)$ mainly relies on the evolution with respect to δ of the standard deviation $\sigma(Z_\delta)$ even though the definition of the CoV makes use of both first and second moments of the property Z_δ. Indeed, when δ increases the first moment $E(Z_\delta)$ tends to the effective property which is non-zero. Therefore its evolution has a small influence on the CoV in comparison to the one of the standard deviation which tends toward zero. Accordingly, this second criterion can be interpreted as a minimal VE size for which the individual fluctuations of the apparent properties are small enough. However the individual fluctuations of the apparent properties are only partially taken into account in this criterion since standard deviations alone are considered.

Fig. 9 reports the evolution with respect to the contrast c of the RVE size δ_{CoV} associated either with the in-plane bulk or shear modulus for different accuracies ($\varepsilon = 2\%, 5\%$) and inclusion volume fractions ($f^I = 15\%, 30\%$). The same trends as those found for the evolution of δ_{BC} are observed. However, the numerical values of δ_{CoV} are larger than those observed for δ_{BC}. These trends show that CoV-based RVE criterion which account for the individual fluctuations of the apparent properties is more demanding than the BC-based RVE criterion which only includes the BC-based fluctuations. Thus, the trends already observed in Section 3.5 for rigidly reinforced composites and porous materials hold for any contrast c. Lastly, it is observed that the RVE size δ_{CoV} is less sensitive to the variations of the inclusion volume fraction than the BC-based RVE criterion δ_{BC}, consistently with results in Figs. 3 and 4.

4.2.2. RVE criterion based on all fluctuation sources

The results established by Hazanov and Huet [31] provide a useful framework to design an RVE criterion taking into account all types of fluctuations. They showed that the apparent moduli tensor $C_\delta^{app}(\omega)$ of a VE $B_\delta(\omega)$ submitted to any

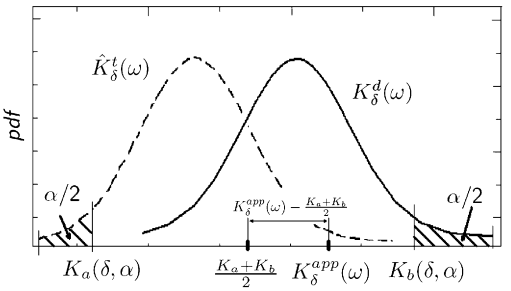

Fig. 10. Graphical illustration of the RVE criterion $\delta_{IF}(K)$.

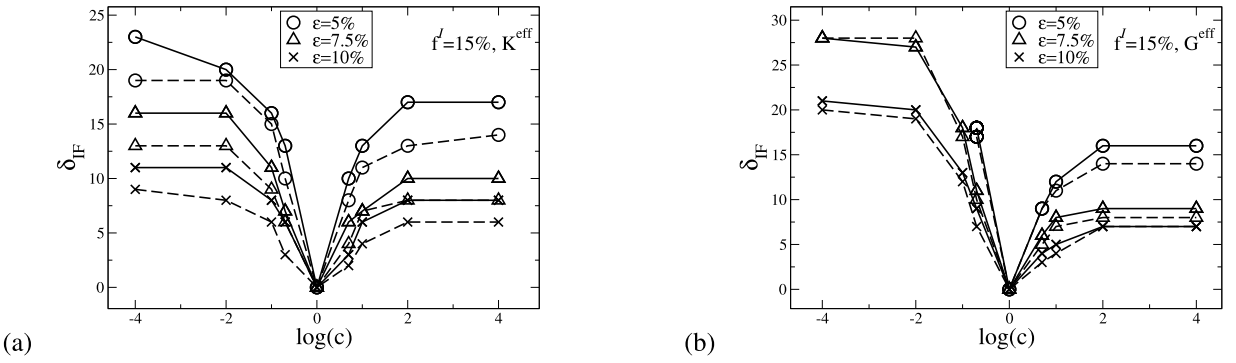

Fig. 11. Variations of the RVE size δ_{IF} associated with the bulk effective modulus (a) or the shear effective modulus (b) with respect to the contrast c for different values of the accuracy ε and probability α. Continuous lines are relative to $\alpha = 5\%$ while dashed curves are related to $\alpha = 10\%$. $f^I = 15\%$.

BC satisfying Hill's macrohomogeneity condition, is bounded by the apparent moduli tensors $C^d_\delta(\omega)$ and $\hat{C}^t_\delta(\omega) = (S^t_\delta(\omega))^{-1}$ associated with the same VE but submitted to ADBC and UTBC respectively, i.e.

$$\hat{C}^t_\delta(\omega) = \left(S^t_\delta(\omega)\right)^{-1} \leqslant C^{app}_\delta(\omega) \leqslant C^d_\delta(\omega) \tag{27}$$

The projection[2] of order relation (27) on J_T and K_T yields

$$\hat{Z}^t_\delta(\omega) \leqslant Z^{app}_\delta(\omega) \leqslant Z^d_\delta(\omega) \quad \text{with} \quad \begin{cases} Z^{app}_\delta(\omega) = \frac{1}{2} J_T : C^{app}_\delta(\omega),\ \hat{Z}^t_\delta(\omega) = \frac{1}{2} J_T : \hat{C}^t_\delta(\omega) & \text{for } Z = K \\ Z^{app}_\delta(\omega) = \frac{1}{4} K_T : C^{app}_\delta(\omega),\ \hat{Z}^t_\delta(\omega) = \frac{1}{4} K_T : \hat{C}^t_\delta(\omega) & \text{for } Z = G \end{cases} \tag{28}$$

The moduli $Z^d_\delta(\omega)$ for $Z = K$ or G in Eq. (28) are already defined in Eq. (14). From Eq. (28), the individual fluctuations of the apparent in-plane moduli $Z^{app}_\delta(\omega)$ might be bounded by making use of the statistical distribution of its lower $\hat{Z}^t_\delta(\omega)$ and upper $Z^d_\delta(\omega)$ bounds which both converge towards the same Dirac distribution at Z^{eff} when δ tends to infinity. Relying on this remark, a third RVE criterion which ensures small individual fluctuations of the apparent moduli may be obtained in the following way. As illustrated in Fig. 10, for a given probability α and VE size δ, both values $Z_a(\delta,\alpha)$ and $Z_b(\delta,\alpha)$ are defined as follows:

$$P\left(\hat{Z}^t_\delta(\omega) \geqslant Z_a(\delta,\alpha)\right) = 1 - \alpha/2, \qquad P\left(Z^d_\delta(\omega) \leqslant Z_b(\delta,\alpha)\right) = 1 - \alpha/2 \tag{29}$$

From the definition (29) of $Z_a(\delta,\alpha)$ and $Z_b(\delta,\alpha)$, an individual fluctuations (IF) type RVE size $\delta_{IF}(Z)$ for an accuracy ε might be defined as

$$\delta_{IF}(Z) = \min_\delta \left\{ \delta,\ \frac{Z_b(\delta,\alpha) - Z_a(\delta,\alpha)}{Z_b(\delta,\alpha) + Z_a(\delta,\alpha)} \leqslant \varepsilon \right\} \tag{30}$$

It is worth noting that the RVE criterion (30) guarantees that at least a proportion $(1-\alpha)$ of the values of $Z^{app}_\delta(\omega)$ are such that $|Z^{app}_\delta(\omega) - \frac{Z_a(\delta,\alpha)+Z_b(\delta,\alpha)}{2}| \leqslant \varepsilon \frac{Z_a(\delta,\alpha)+Z_b(\delta,\alpha)}{2}$ for $\delta > \delta_{IF}(Z)$ thus ensuring small individual fluctuations of the apparent modulus $Z^{app}_\delta(\omega)$.

Fig. 11 (resp. Fig. 12) reports the evolutions of the RVE size δ_{IF} for both the in-plane bulk and shear moduli as functions of the contrast at $f^I = 15\%$ (resp. $f^I = 30\%$). Different values of the probability ($\alpha = 5\%, 10\%$) and accuracy ($\varepsilon = 5\%, 7.5\%, 10\%$)

[2] It can easily be shown that inequalities are conserved after projection.

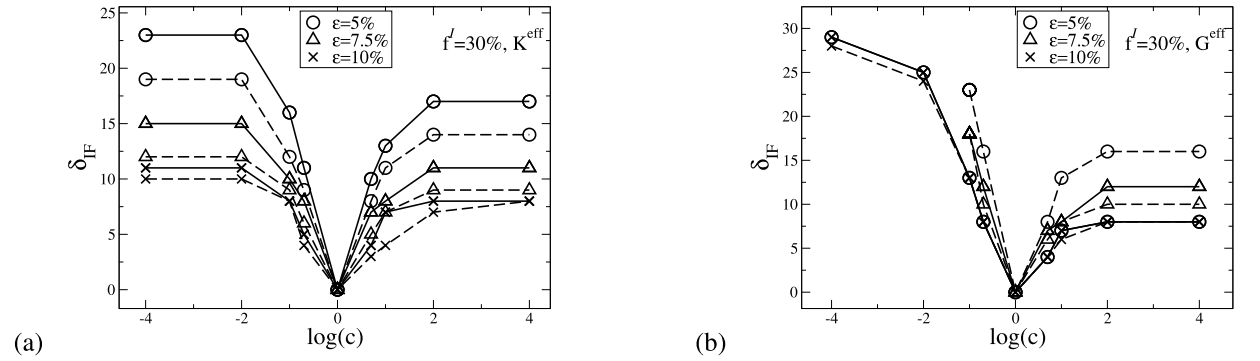

Fig. 12. Variations of the RVE size δ_{IF} associated with the bulk effective modulus (a) or the shear effective modulus (b) with respect to the contrast c for different values of the accuracy ε and probability α. Continuous lines are relative to $\alpha = 5\%$ while dashed curves are related to $\alpha = 10\%$. $f^I = 30\%$.

are considered. It should be noted that the minimum value of the accuracy — namely $\varepsilon = 5\%$ — has been chosen in order that RVE sizes lesser than $\delta = 30$ might be attained when the δ_{IF} RVE criterion is applied to the rigidly reinforced composite and porous material. As shown in these figures, the same trends as the ones found for both former RVE criteria δ_{BC}, δ_{CoV} are observed (see Sections 4.1 and 4.2.1). However, the values of δ_{IF} when compared to the ones found for δ_{BC}, δ_{CoV} — for both the same and only shared accuracy ($\varepsilon = 5\%$) and the same contrasts and inclusion volume fractions — are significantly larger. Therefore, the δ_{IF} criterion is as expected the most demanding criterion among the three RVE criteria presented in this paper. Ratios between δ_{IF} and δ_{CoV} for similar conditions and for $\varepsilon = 5\%$ are of the order of 2.

5. Conclusion

A statistical study of the apparent properties of random fiber–matrix composites with infinite contrasts has been performed by means of a new numerical procedure established by Salmi et al. in [18]. Relying on the quantities considered in this study — i.e. $CoV(Z), pdf(Z), \Delta Z^{VOR}/Z$ — and their evolutions with respect to the VE size, three proposals of RVE size criteria have been presented. The first one, which aims at determining a "computational RVE" size, only allows for the BC-based fluctuations. A rigorous probabilistic interpretation might be ascribed to this criterion by the incorporation into its definition of a statistical confidence interval linked to the statistical fluctuations of the apparent behavior and the number of realizations. The second and third RVE size criteria are more explicitly based on the fluctuations of apparent properties. The second one only takes into account the individual fluctuations of the microstructure through the coefficient of variations of the apparent behaviors. The last RVE criterion, designed with the point of view of substituting a heterogeneous material by a homogeneous equivalent one in structural calculations, accounts for both the whole statistics of the individual fluctuations through the pdfs of the apparent properties and the BC-based fluctuations since discrepancies between ADBC and UTBC are considered in its definition (30). Numerical applications of these criteria to random fiber–matrix composites for two values of the fiber volume fraction ($f^I = 15\%, 30\%$) and contrasts ranging from $c = 10^{-4}$ to $c = 10^4$ show that the equivalent medium-based criterion is the most demanding criterion while the BC-based criterion is the less demanding one. Ratios between RVE sizes defined according to these three definitions for similar composites and accuracy levels can be of the order of five or even more.

Lastly, although the statistics of the apparent behavior are of primal use to evaluate RVE sizes, they can also be employed in situations where there is no RVE — e.g. when the material microstructure is not stationary — or when the separation of scale assumption is not fulfilled. For instance, to illustrate such a point of view, it has been seen in Section 3.5.2 that the pdfs of the apparent moduli quickly converge towards Gaussian distributions. Such a result may be very interesting when the convergence towards the effective property occurs for a value of δ, say δ_{RVE}, larger than the one, say δ_{pdf}, associated with the convergence of the pdfs of the apparent moduli towards a Gaussian-shaped distribution. Indeed, for such situations, if the separation of scale assumption is not satisfied for a given structural mechanics problem — in the sense that the RVE size is too large in comparison with the size of the structure and the characteristic fluctuation lengths of the macroscopic fields generated in it — it may be possible to solve this problem — e.g., by means of stochastic numerical schemes such as the Stochastic Finite Elements Method [32] — by making use of VEs of size δ_{pdf} for which the distributions of their apparent properties are Gaussian. Of course, the size δ_{pdf}, which is smaller than the RVE size, should also be small enough in comparison with the size of the structure to enable structural calculations. The values of the expectation and standard deviation of the apparent moduli distributions, which fully characterize the Gaussian distributions, can be obtained by performing a statistical study of the apparent properties at $\delta = \delta_{pdf}$.

Acknowledgements

M.B. and F.A. gratefully acknowledge Professor André Zaoui for all the fruitful and valuable discussions, exciting works, constant support and very pleasant times shared with him during numerous years.

References

[1] K. Hill, Elastic properties of reinforced solids: Some theoretical principles, Journal of the Mechanics and Physics of Solids 11 (1963) 357–372.
[2] Z. Hashin, Analysis of composite materials, Journal of Applied Mechanics 50 (1983) 481–505.
[3] M. Ostoja-Starzewski, Material spatial randomness: From statistical to representative volume element, Probabilistic Engineering Mechanics 21 (2006) 112–132.
[4] E. Sanchez-Palencia, Non-Homogeneous Media and Vibration Theory, Lecture Notes in Physics, vol. 127, Springer Verlag, Berlin–New York, 1980.
[5] G.C. Papanicolaou, S.R.S. Varadhan, Rigorous results in statistical mechanics in quantum field theory, in: J. Fritz, J.L. Lebowitz, D. Szasz (Eds.), Colloquia Mathematica Societatis Janos Bolyai, North-Holland, Amsterdam, 1978, pp. 835–873.
[6] K. Sab, On the homogenization and the simulation of random materials, European Journal of Mechanics A/Solids 11 (1992) 585–607.
[7] W.J. Drugan, J.R. Willis, A micromechanics-based nonlocal constitutive equation and estimates of representative volume element size for elastic composites, Journal of the Mechanics and Physics of Solids 44 (1996) 497–524.
[8] L. Monetto, W.J. Drugan, A micromechanics-based nonlocal constitutive equation for elastic composites containing randomly oriented spheroidal heterogeneities, Journal of the Mechanics and Physics of Solids 52 (2004) 359–393.
[9] L. Monetto, W.J. Drugan, A micromechanics-based nonlocal constitutive equation and minimum RVE size estimates for random elastic composites containing aligned spheroidal heterogeneities, Journal of the Mechanics and Physics of Solids 57 (2009) 1578–1595.
[10] A. Gusev, Representative volume element size for elastic composites: A numerical study, Journal of the Mechanics and Physics of Solids 45 (1997) 1449–1459.
[11] M. Ostoja-Starzewski, Random field models of heterogeneous materials, International Journal of Solids and Structures 35 (1998) 2429–2455.
[12] J. Segurado, J. Llorca, A numerical approximation to the elastic properties of sphere-reinforced composites, Journal of the Mechanics and Physics of Solids 50 (2002) 2107–2121.
[13] T. Kanit, S. Forest, I. Galliet, V. Mounoury, D. Jeulin, Determination of the size of the representative volume element for random composites: statistical and numerical, International Journal of Solids and Structures 40 (2003) 3647–3679.
[14] I.M. Gitman, M.B. Gitman, H. Askes, Quantification of stochastically stable representative volumes for random heterogeneous materials, Archive of Applied Mechanics 75 (2006) 79–92.
[15] C. Pelissou, J. Baccou, Y. Monerie, F. Perales, Determination of the size of the representative volume element for random quasi-brittle composites, International Journal of Solids and Structures 46 (2009) 2842–2855.
[16] J. Escoda, F. Willot, D. Jeulin, J. Sanahuja, C. Toulemonde, Estimation of local stresses and elastic properties of a mortar sample by FFT computation of fields on a 3D image, Cement and Concrete Research 41 (2011) 542–556.
[17] I.M. Gitman, H. Askes, L.J. Sluys, Representative volume: Existence and size determination, Engineering Fracture Mechanics 74 (1996) 2518–2534.
[18] M. Salmi, F. Auslender, M. Bornert, M. Fogli, Apparent and effective mechanical properties of linear matrix–inclusion random composites: improved bounds for the effective behavior, International Journal of Solids and Structures (2012), in press, http://dx.doi.org/10.1016/j.ijsolstr.2012.01.018.
[19] C. Huet, Application of variational concepts to size effects in elastic heterogeneous bodies, Journal of the Mechanics and Physics of Solids 38 (1990) 813–841.
[20] M. Danielsson, D. Parks, M. Boyce, Micromechanics, macromechanics and constitutive modeling of the elasto-viscoplastic deformation rubber-toughened glassy polymers, Journal of the Mechanics and Physics of Solids 55 (2007) 533–561.
[21] M. Ostoja-Starzewski, P.Y. Sheng, K. Alzebdeh, Spring network models in elasticity and fracture of composites and polycrystals, Computational Materials Science 7 (1996) 82–93.
[22] N. Bilger, F. Auslender, M. Bornert, J.-C. Michel, H. Moulinec, P. Suquet, A. Zaoui, Effect of nonuniform distribution of voids on the plastic response of voided materials: a computational and statistical analysis, International Journal of Solids and Structures 42 (2005) 517–538.
[23] C. Stolz, A. Zaoui, Analyse morphologique et approches variationnelles du comportement d'un milieu élastique hétérogène, Comptes Rendus de l'Académie des Sciences II 312 (1991) 143–150.
[24] M. Bornert, C. Stolz, A. Zaoui, Morphologically representative pattern-based bounding in elasticity, Journal of the Mechanics and Physics of Solids 44 (1996) 307–331.
[25] M.D. Rintoul, S. Torquato, Reconstruction of the structure of dispersions, Journal of Colloid and Interface Science 186 (1997) 467–476.
[26] F. Willot, Y.P. Pellegrini, P.P. Castaneda, Localization of elastic deformation in strongly anisotropic, porous, linear materials with periodic microstructures: Exact solutions and dilute expansions, Journal of the Mechanics and Physics of Solids 56 (2008) 1245–1268.
[27] J.D. Eshelby, The determination of the elastic field of an ellipsoidal inclusion and related problems, Proceeding of the Royal Society A 421 (1957) 376–396.
[28] F. Willot, D. Jeulin, Elastic behavior of composites containing Boolean random sets of inhomogeneities, International Journal of Engineering Science 47 (2009) 313–324.
[29] G. Casella, R.L. Berger, Statistical Inference, Duxbury Press, United States, 2001.
[30] V. Blanc, Modélisation du comportement thermomécanique des combustibles à particules par une approche multi-échelle, PhD thesis, Université de Provence, 11 décembre 2009.
[31] S. Hazanov, C. Huet, Order relationships for boundary conditions effect in heterogeneous bodies smaller than the representative volume, Journal of the Mechanics and Physics of Solids 42 (1994) 1995–2011.
[32] R.G. Ghanem, P.D. Spanos, Stochastic Finite Elements: A Spectral Approach, Dover Publications, 1991.